THE CHALLENGES OF THE LIPAc CIRCULATORS TOWARD HIGH DUTY CYCLE

K. Hirosawa[1*], N. Kubo, T. Sasaki, W. Abe, K. Kondo[1], QST, Rokkasho, Japan
F. Scantamburlo[1], I. Moya[1], Y. Carin[1], F4E, Garching, Germany
J-P. Adam, CEA, Paris, France
L. González-Gallego, IFMIF-DONES España, Granada, Spain
[1]also at IFMIF/EVEDA PT, Rokkasho, Japan

Abstract

The Linear IFMIF Prototype Accelerator (LIPAc) is a deuteron accelerator that aims to accelerate the 125 mA beam up to 9 MeV in the continuous wave (CW) operation mode. The objective of the facility is validation of technological and scientific aspects of the base design and to clarify the further challenges towards the 40 MeV-125 mA-CW deuteron beam for the accelerator part. The RF system of the LIPAc is designed to provide 1.2 MW power in total to the RFQ, driven by eight amplification lines up to 200 kW per station. The SRF-RF system is also the same tetrode system, but only the power level is lower than the RFQ system. In the present operation scenario, we are working to increase the duty cycle under the same beam current until CW operation. Thus, the compensation control of the dissipation for RF devices during beam commissioning is one of the core challenges in our project. In the report, we summarize the test results and the analysis with comparisons between the existing and the new circulator.

INTRODUCTION

The radio-frequency (RF) system for the Linear IFMIF Prototype Accelerator (LIPAc) was originally designed to support continuous wave (CW) high-power operation, with the objective of accelerating a 125 mA deuteron beam [1]. The RFQ cavity exhibits a wall power loss, approximately 560 kW, and RF power is supplied via eight synchronized RF stations utilizing the White Rabbit protocol for precise timing and control.

To compensate the maximum beam-induced voltage, the RF system is configured to deliver nearly twice the power required for stand-alone operation. Consequently, each RF station is capable of transmitting approximately 80 kW under no beam-loading conditions and up to 160 kW when beam loading is present.

However, other subsystems—such as the RFQ cavity and the injector—are not inherently compatible with variable beam current operation under CW conditions. Therefore, several components have been modified to support pulsed operation. These include the low-level RF (LLRF) control system, solid-state amplifiers rated below 300 kW, and power supplies for the two-stage tetrode amplifier system rated below 200 kW. These adaptations could accept flexible combinations of pulse length and repetition rate, albeit as post-design modifications.

Despite these improvements, managing high-power operation under variable duty cycles remains challenging, particularly for components such as the circulator and the RFQ cavity. The RF resonance characteristics of the circulator is highly sensitive to thermal conditions specifically, the temperature of soft-ferrite materials and the internal geometry of the cavity. In DC-mode operation with significant beam loading, variable power dissipation introduces complexity from the perspective of thermal time constants.

This report presents insights gained from previous circulator designs and discusses key scientific considerations relevant to future high-duty cycle operations.

LIPAc RF SYSTEM

The appearance of the LIPAc RF system is shown in Fig. 1.

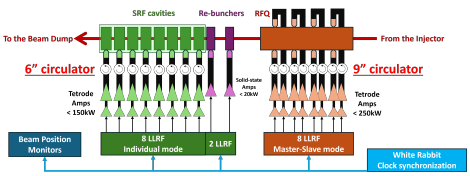

Figure 1: A schematic drawing of the LIPAc RF system.

The initial stage of acceleration in the LIPAc system is performed through a radio-frequency quadrupole (RFQ) cavity. The LIPAc RFQ is a 9.8-meter-long resonator, powered by eight RF power stations and corresponding couplers. Due to this configuration, each RF station must accommodate peak power levels exceeding the nominal output of a single station. Consequently, the circulator must be capable of handling and maintaining stability under high peak power conditions, typically in the range of 400 kW to 600 kW.

The second acceleration stage is implemented via a superconducting radio-frequency (SRF) linear accelerator, which comprises eight superconducting half-wave resonators (SRF cavities). Each SRF cavity operates as an independent unit, resulting in a relatively straightforward system configuration. However, during warm conditioning or machine operation without beam loading, the input RF power is fully reflected back to the RF station. In such scenarios, precise matching of the resonance curve within the circulator is critical to

* hirosawa.koki@qst.go.jp

minimize external impedance drift for the tetrode output cavity and to ensure its protection.

Although the specific roles of the circulator differ between the RFQ and SRF systems, their importance is equally significant in both contexts. The most significant challenge unique to the LIPAc system lies in the requirement to regulate thermal dynamics under arbitrary beam current and duty cycle conditions, particularly in preparation for continuous wave (CW) operation. Accordingly, the circulator must be carefully designed and tuned to meet the distinct operational demands of each acceleration stage and operation mode.

Here, the buncher system is also used between the RFQ and the SRF. It works to shape the beam in longitudinal phase space without energy exchange. Because individual mode and solid-state amplification system is adopted for the RF driver, the stand-alone circulator was not prepared.

LIPAc CIRCULATOR

The circulator is implemented to prevent unacceptable levels of reflected power from resonators with high quality factors (Q). A schematic of the RF amplification system is drawn in Fig. 2, which explains the circulator works as the isolator between the tetrode output cavity and the accelerating cavity of LINAC.

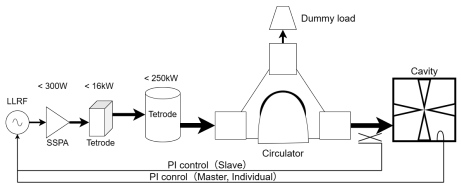

Figure 2: A schematic drawing of the LIPAc RF amplification line.

As previously described, the circulator functions to redirect and dissipate surplus RF power. This behavior is fundamentally originated in the interaction between the spin of electrons and the alternating RF magnetic field within a medium such as soft ferrite. The applicable transmission line structure varies depending on the operating frequency band. For lower frequency bands—such as the 175 MHz used in the LIPAc RF system—a coaxial transmission line structure is more appropriate. Accordingly, a Y-stripline circulator configuration is considered a suitable and practical solution for this frequency range. Figure 3 illustrates a simplified structural diagram of the Y-stripline circulator. The circulator's operational characteristics are determined by the applied direct current (DC) magnetic field and the biased soft-ferrite material surrounding the central stripline [2].

The solution to Maxwell's equations within the ferrite medium requires appropriate values for the relative permittivity and permeability. The relative permeability tensor, denoted as $\bar{\mu}_r$, is expressed as the sum of the identity matrix $\bar{I}$ and the magnetic susceptibility tensor $\bar{\chi}$:

$$\bar{\mu}_r = \bar{I} + \bar{\chi},$$

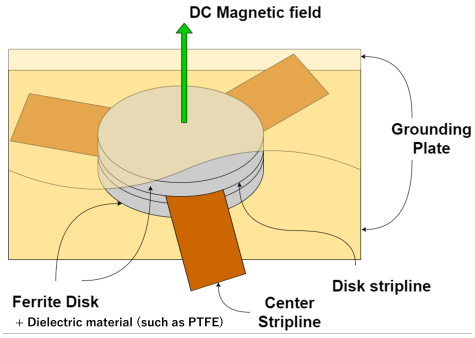

Figure 3: An example structure of the Y-stripline circulator.

When a magnetic bias field is applied along the z-axis, the relative permeability tensor takes the following form:

$$\bar{\mu}_r = \begin{pmatrix} \mu & -i\kappa & 0 \\ i\kappa & \mu & 0 \\ 0 & 0 & 1 \end{pmatrix}.$$

The susceptibility tensor $\bar{\chi}$ is defined as:

$$\bar{\chi} = \begin{pmatrix} \chi_{xx} & \chi_{xy} & 0 \\ \chi_{yx} & \chi_{yy} & 0 \\ 0 & 0 & 1 \end{pmatrix},$$

with its components given by:

$$\begin{cases} \chi_{xx} = \chi_{yy} = \dfrac{\omega_m \omega_i}{\omega^2 + \omega_i^2} \\ -\chi_{xy} = \chi_{yx} = \dfrac{i\omega_m \omega}{-\omega^2 + \omega_i^2} \end{cases}$$

The angular frequencies involved are defined as follows:

$$\begin{cases} \omega_{\mathrm{m}} = \gamma M_0 \quad [\mathrm{rad/s}] \\ \omega_{\mathrm{i}} = \gamma (H_0 - N_z M_0) \quad [\mathrm{rad/s}] \end{cases}$$

Here, the parameters used above are defined as:

M_0 : the saturation magnetization [A/m]

γ : the gyromagnetic ratio = 2.21×10^5 [(rad/s) / (A/m)]

ω : the radian frequency [rad/s]

μ_0 : the free space permeability [$4\pi \times 10^{-7}$ H/m]

H_0 : the applied direct magnetic field intensity [A/m]

N_z : a z-directed shape demagnetization factor of the geometry

Among these parameters, the saturation magnetization M_0 denotes temperature dependence, which is directly related to the thermal dynamics of the circulator in the context of this study.

Table 1: Specification Requirements of the Circulator

Items	nominal	in range
Frequency	175 MHz	300 kHz
Power	160 kW	0 – 230 kW
Duty cycle	100% (CW)	0 – 100%
$S_{11,22,33}$	−26 dB	−20 dB
$S_{12,23,31}$	−26 dB	−20 dB
$S_{21,32,13}$	−0.15 dB	−0.15 dB

Requirements

The circulator requirement is listed in Table 1.

The LIPAc project aims to achieve 125 mA continuous wave (CW) operation—a highly ambitious objective that presents considerable challenges. This goal is unlikely to be attained in a single step or through a limited number of incremental operation steps, due to the substantial power dissipation associated with RF transmission and variable duty cycles. Despite the complexity and ambition of the project, the original circulator model has been reported to exhibit numerous deficiencies. The design contains several issues—both in hardware and software—that are considered problematic.

Original model

Following problems has been found for 4 years from 2021 to 2025. The analyzed route cause is simply explained after the symbol ∵ for each item.

Issues on the hardware As the hardware issue,

- Discharge because of the loosen connection in the coaxial transition. ∵ Difference of the thermal cycle among bolts(SUS304), inner transition(Al), and Y-stripline(Cu).
- Water leak from internal cooling water line. ∵ Aging degradation of the atmospheric welding in the strong electromagnetic environment.
- Electro magnetic radiative noise from the circulator ports. ∵ Hole and pipe size is near to the coaxial line ratio, unfortunately.
- Interaction between pair circulators because of the magnetic leakage. ∵ Return yoke by the magnetic metal is not implemented.
- Unstable coil current driver. ∵ Power supply is poor quality for the normal motor, and the cable is poorly EMC insulated.
- High temperature > 160 °C due to the large resistivity of the coil. ∵ Less examination in the factory in the past or aging effect.

Figure 4 presents an image of the damaged internal transition between the coaxial inner conductor and the stripline. This region represents the structurally weakest point within the circulator geometry, as the transition serves two simultaneous functions: providing RF contact and mechanically supporting internal components. The most critical issue identified is that the inner stripline of the circulator is secured by only two bolts. Through investigation, we identified the cause of the burnt related to the material properties of the bolts. Specifically, the difference in the coefficients of thermal expansion between the bolt material and surrounding components contributed to a gradual loosening of the fastening under thermal cycling. To mitigate this issue, the original stainless steel bolts were replaced with brass bolts, which denotes more favorable thermal compatibility. The integrity of the fastening is now monitored periodically, particularly during long operational periods.

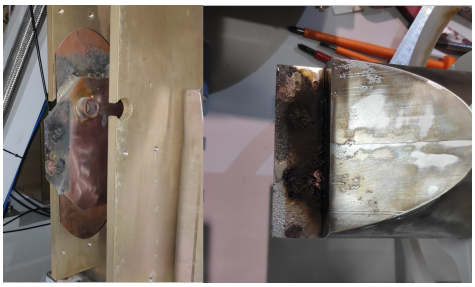

Figure 4: Pictures of the broken stripline (left) and the inner transition (right).

Issues on the RF characteristics As the software issue, which means that the problem related with the frequency characteristics.

- Large mismatch among S-parameters. ∵ Less quality control of the manufacturing.
- Demagnetization because of the coil heating. ∵ Requirement of the large compensation magnetic field and less quality control of the manufacturing.
- Long transient time for the thermal drift. ∵ Normally not the problem, but it is unwelcome for the requirement of our challenging project.
- Input/output balance change when the duty cycle changes ∵ It is also not a problem for normal case, it is just for the challenge of our project.

With regard to the matching among the S-parameters, it is essential to align the resonance peaks with respect to the coil current dependency. However, the original circulator models has substantial mismatches in this regard. Figure 5 introduces two samples of the measured S-parameter characteristics at 175 MHz for various driving coil currents. The primary issue is the absence of a clearly defined optimal operating point, compounded by the fact that this behavior may vary as the average power dissipation increases. In order to control the circulator as a passive device from the RF system perspective, its response must remain consistent and

well-matched. This consistency must be maintained even under significant variations in duty cycle, provided that the calibration setup is kept.

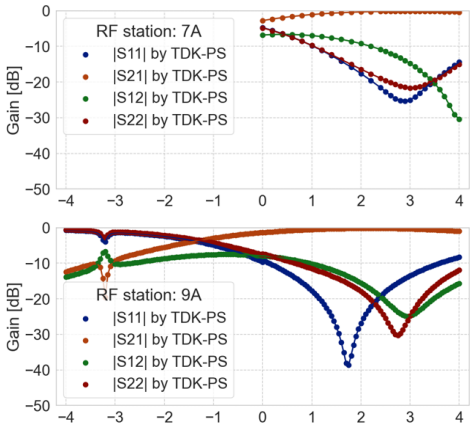

Figure 5: Coil current dependencies of the circulator S-parameters at 175 MHz for two different circulators.

Another issue is the demagnetization caused by the coil heating without RF injection, which is a difficult situation to be resolved easily. Figure 6 illustrates the thermal drift observed in the S-parameters when the coil current is applied at its optimal operating point over a two-hour period. Under the initial conditions, the surface temperature was 25 °C. After two hours of operation, the surface temperatures reached 117 °C on the compensation coil and 56 °C on the biased permanent magnet, as shown in Fig. 7. These thermal variations highlight the importance of temperature management to provide stable RF performance.

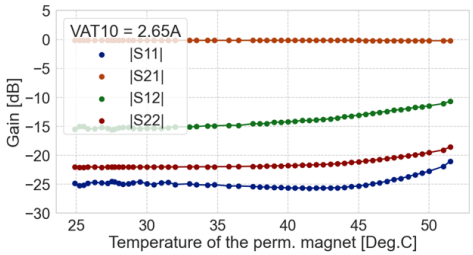

Figure 6: S-parameter drift when coil current set to the its optimum point for two hours.

As the solution for issues mentioned above, we decided to replace the circulator model with the new improved model.

Revised model

The prototype of the revised model has been manufactured in FY2024 [3]. The new model has many improvements and well adjusted for the coil current dependency.

Improvements Especially for the RF characteristics point of view, following improvements were done as listed in below.

- Improved the thermal conductivity to make the transient of the dissipation quick.

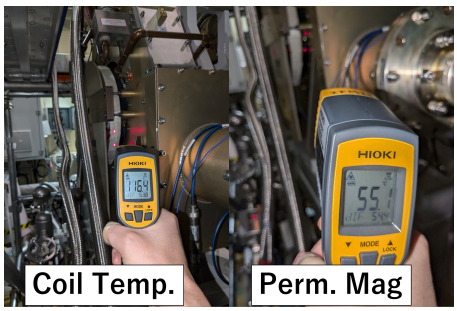

Figure 7: Surface temperature of the compensation coil and a permanent magnet after 2 hours from coil driver set to the optimum.

- Located the coil on the heat sink with the housing to remove the temperature increasing of the coil.
- Brazed the inner transition and the copper stripline to make the connection sure and to avoid the micro discharge between them.
- Made the return path by the 20 mm thick steel plates for DC magnetic bias field and remove a coil located in the side of back-to-back to mitigate the coupling of between the pair circulator.
- Reduce the resistivity of the coil to reduce the coil heating.
- Removed the welding part from the water pipes to repair it easily, and improved water cooling circuit.

Figure 8 shows that the result of the S-parameter measurement of the coil current dependency for the new circulator. This result told us that the S_{11} resonance is the optimum point and −35 dB isolation is achieved for all at that point. This means that it is easier to implement the automatic control loop for the circulator if we choose the operation point at the S_{11} resonance.

Control software Instead of the gain control, the relative phase between input and output power was chosen under the assumption that S_{11} is dominant component. Then, PI control can be used to follow the circulator temperature change. Figure 9 illustrates the schematic of the block diagram of the implemented PI control loop. As a preliminary test, feedback is developed in the laptop by python via EPICS PV. In fact, it already works well because the circulator compensation coil speed should be negligibly slow compared with the main feedback loop of the low-level RF control system.

By using this controller, the high-power test of the new circulator has been conducted and validated the function. Figure 10 shows the result of the automatic control for the variable dissipation several power level changed from 60 kW to 210 kW in the CW mode. We successfully demonstrated the circulator and the software performance. On the other hand, it was found that the reflection level is changed even

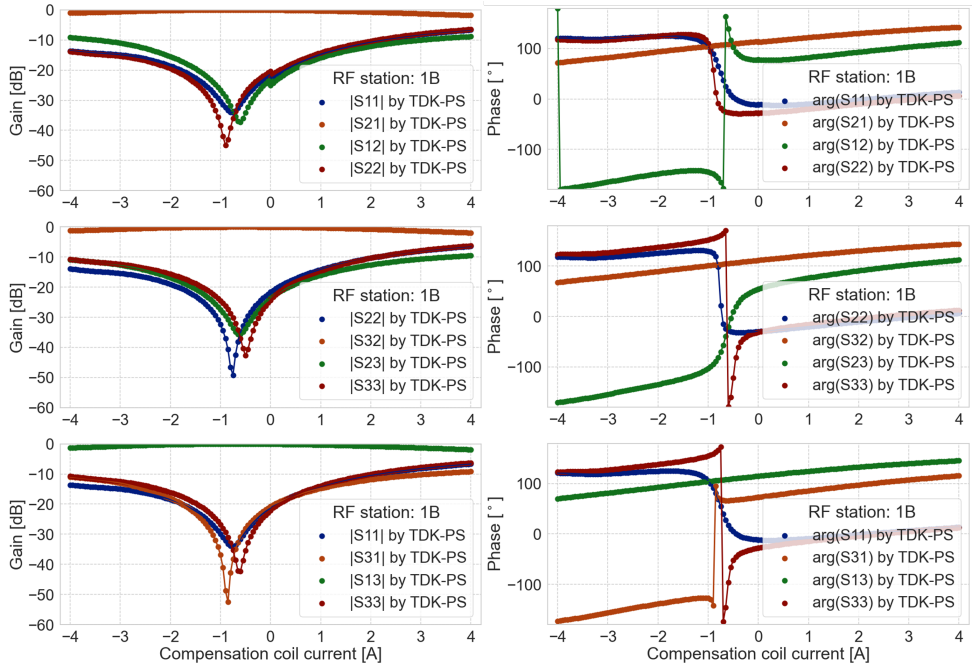

Figure 8: Measured coil current dependency of the S-Parameter for the new circulator.

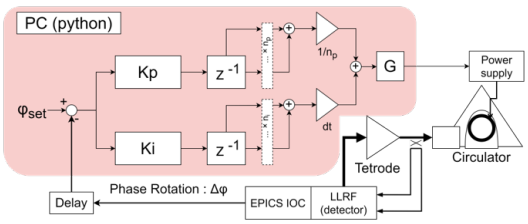

Figure 9: A schematic of the control feedback loop of the new circulator coil current.

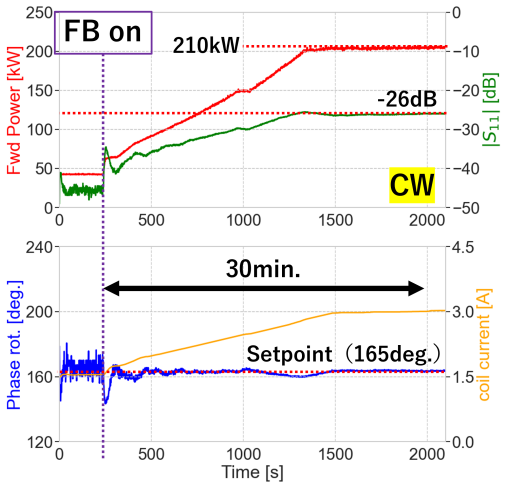

Figure 10: The result of the high-power test of the new circulator with the developed PI controller.

if the relative phase is kept in the same value. This result may indicate the resonance drift is not negligible in the high-power case. If it is coming from the principle, the reason is M_0 change for ω_i can be canceled by compensating H_0, but it is not contributed for ω_m. The possibility of the isolation drift for the directional coupler is still in the candidate list, and so we plan to study them in more detail.

CONCLUSION

LIPAc has many challenges, and the management of the dissipation toward the 125 mA-CW beam acceleration level is one of core topics. The circulator, a key component of the RF system, of the existing model has many difficulties for the high-power and CW operation. Accordingly, we decided to replace the circulator with the new model. The new model has been improved and has solutions for most of the issues we found in the existing model, and the new specification has been improved impressively. To prepare for the future situation with a large dissipation, a new circulator control software was also developed. With the new software, the high-power characteristics of the prototype has been successfully demonstrated. As the next plan, we are going to replace the all circulator with the new model. With regard to the control software, we will implement it in the LLRF control system to synchronize it with the arbitral pulse condition from low duty cycle to the CW.

REFERENCES

[1] Purificacion Mendez *et al.*, "*LIPAc RF power system: design and main practical implementation issues*", Fusion Engineering and Design, Vol. 165, pp. 112226, 2021.

[2] Joseph Helszajn, "*The Stripline Circulator: Theory and Practice*", John Wiley & Sons, 2008.

[3] Microwave Techniques, https://www.microwavetechniques.com/